ELSEVIER

Coastal Engineering 46 (2002) 277–289

Coastal Engineering
An International Journal for Coastal, Harbour and Offshore Engineers

www.elsevier.com/locate/coastaleng

Regeneration of sand waves after dredging

M.A.F. Knaapen *, S.J.M.H. Hulscher

Department of Civil Engineering, University of Twente, P.O. Box 217, 7500 AE Enschede, The Netherlands

Received 6 September 2001; received in revised form 14 May 2002; accepted 7 June 2002

Abstract

Sand waves are large bed waves on the seabed, being a few metres high and lying hundreds of metres apart. In some cases, these sand waves occur in navigation channels. If these sand waves reduce the water depth to an unacceptable level and hinder navigation, they need to be dredged. It has been observed in the Bisanseto Channel in Japan that the sand waves tend to regain their shape after dredging. In this paper, we address modelling of this regeneration of sand waves, aiming to predict this process. For this purpose, we combine a very simple, yet effective, amplitude-evolution model based on the Landau equation, with measurements in the Bisanseto Channel. The model parameters are tuned to the measured data using a genetic algorithm, a stochastic optimization routine. The results are good. The tuned model accurately reproduces the measured growth of the sand waves. The differences between the measured weave heights and the model results are smaller than the measurement noise. Furthermore, the resulting parameters are surprisingly consistent, given the large variations in the sediment characteristics, the water depth and the flow field. This approach was tested on its predictive capacity using a synthetic test case. The model was tuned based on constructed predredging data and the amplitude evolution as measured for over 2 years. After tuning, the predictions were accurate for about 10 years. Thus, it is shown that the approach could be a useful tool in the optimization of dredging strategies in case of dredging of sand waves.

Keywords: Sand waves; Dredging; Landau equation; Optimization; Morphology

1. Introduction

As modern ships require increased navigation depth, more and more harbour authorities are forced to dredge the entrance channels to their harbours. In a number of navigation channels, sand waves limit the depth of these channels (Katoh et al., 1998; Van Maren, 1998).

Seabed sand waves are elongated rhythmic bed features spaced about 100–800 m apart and several metres high. Sand waves are found in shallow tidal seas all over the world (Ludwick, 1972; Boggs, 1974; Field et al., 1981; Aliotta and Perillo, 1987; Harris, 1988; Huntley et al., 1982; Ikehara and Kinoshita, 1994; Katoh et al., 1998). In some cases, sand waves occur superimposed on large scale features such as tidal sand banks (Lanckneus and De Moor, 1991), shoreface-connected ridges (Van de Meene and Van Rijn, 2000) or individual shoals (Katoh et al., 1998).

Besides the practical interest, sand waves are also interesting from a scientific point of view. It is

* Corresponding author.
E-mail address: m.a.f.knaapen@ctw.utwente.nl (M.A.F. Knaapen).

0378-3839/02/$ - see front matter © 2002 Elsevier Science B.V. All rights reserved.
PII: S0378-3839(02)00090-X

assumed that the sand waves are free instabilities of the system of an erodible bed and the tidal flow over it (Hulscher, 1996; Komarova and Hulscher, 2000; Gerkema, 2000). Sand waves only occur in seas, where the bed consists of noncohesive sand (percentage silt less than 15%, gravel less than 5%) (Terwindt, 1971; Langhorne, 1973; Bokuniewicz et al., 1977; Hulscher and Van Den Brink, 2001). Furthermore, the tidal motion has to be strong, the maximum tidal velocity should be between 0.4 and 1 m/s (Stride, 1982; Amos and King, 1984).

It is shown that a stability analysis helps to explain the generation of sand waves. Furthermore, this approach can be used to estimate in which regions sand waves can be found (Hulscher and Van Den Brink, 2001). The consequence of the sand waves being free instabilities is that they tend to recover after dredging. This phenomena has been observed and monitored by Katoh et al. (1998). At this moment, we do not have a validated model to simulate this process sufficiently accurate.

To keep the navigation channels sufficiently deep, dredging has to take place. The consequences of these dredging activities depends on the dredging strategy. In the Bisanseto Sea, a field of sand waves has been topped off. Katoh et al. (1998) showed that the sand waves regenerate in several years time. The costs of repeated dredging are high and the responsible authorities want to minimize these costs. To minimize the dredging costs, it is crucial to know the rate at which the sand waves regain their original shape.

In the past, a number of sand wave models have been developed (Fredsøe and Deigaard, 1992; O'Conner, 1992; Hulscher, 1996). However, none of these models can describe the complete range of sand wave growth from generation to their final amplitude. In principle, this range is covered in the model derived from basic physical principles by Komarova and Newell (2000). Their approach resulted in a model that consists of two coupled evolution equations of the Ginzburg–Landau type. This model describes sand waves superimposed on large-scale undulations. However, this model is too complex to solve, so that model results cannot be compared to observations.

The stationary equivalent of the Ginzburg–Landau equation was postulated by Landau and Ginzburg (1965). It is a descriptor of the modulations of instabilities in systems that are described by a set of nonlinear partial differential equations. Examples of such problems are the Rayleigh–Bénard convection (Bénard, 1900), Poiseullle flow (Stewartson and Stuart, 1971), Taylor–Couette flow (DiPrima and Swinney, 1981), reaction–diffusion processes (Kuramoto, 1984) and alternate bar behaviour in rivers (Schielen et al., 1993).

We choose a different approach to arrive at a prediction model. If the long spatial modulations of the sand waves are neglected, the model of Komarova and Newell (2000) reduces to the Landau equation:

$$\frac{\partial A}{\partial \tau} = \alpha_0 A - \alpha_1 |A|^2 A \tag{1}$$

$$\tau = \frac{t}{T} \tag{2}$$

in which the dimensionless amplitude A of an arbitrary wave is a function of τ. The parameters determine the solution of the equation: α_0 gives the linear growth rate while α_1 determines the magnitude of the nonlinear term, which counteracts the linear growth. If both parameters are real values ($\in \mathbb{R}$), the ratio $\sqrt{\frac{\alpha_0}{\alpha_1}}$ determines the amplitude of the waves in infinity.

To test this model, it is compared with the data measured in the Bisanseto experiment. The model parameters will be estimated using data assimilation. A genetic algorithm is used to fit the model to the data. This fitting can provide the coefficients in the Landau equations for any specific case.

Fig. 1. The Seto Sea in Japan. The white box in the image points out the Bisanseto Channel in the Seto Sea.

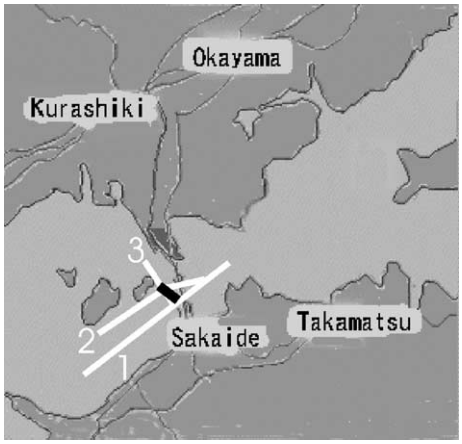

Fig. 2. The black rectangle denotes the sounding area in the Bisanseto Channel. The white lines denote (1) the southern channel, (2) the northern channel, (3) the connection channel.

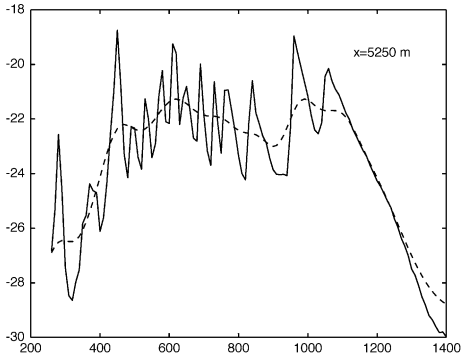

Fig. 4. The depth profile in the northern channel.

In Section 2, the available data from the field experiment in the Bisanseto Channel are described. The sand wave growth model is explained in Section 3. This model will be tuned to fit the data using a genetic algorithm; that is explained in Section 4. The results of this hindcast are given in Section 5, and in Section 6, the predictive capacity is tested. Possible applications of the model are given in Section 7, before the final conclusions in Section 8.

2. Measurements

In this investigation, measurements from a Japanese field experiment in the Seto Sea are used. In 1985, a large experiment was started in the Bisanseto Channel near Kobe (see Fig. 1). The Bisanseto Channel connects the western part of the Seto Sea with the eastern part. In this bottleneck of navigation routes

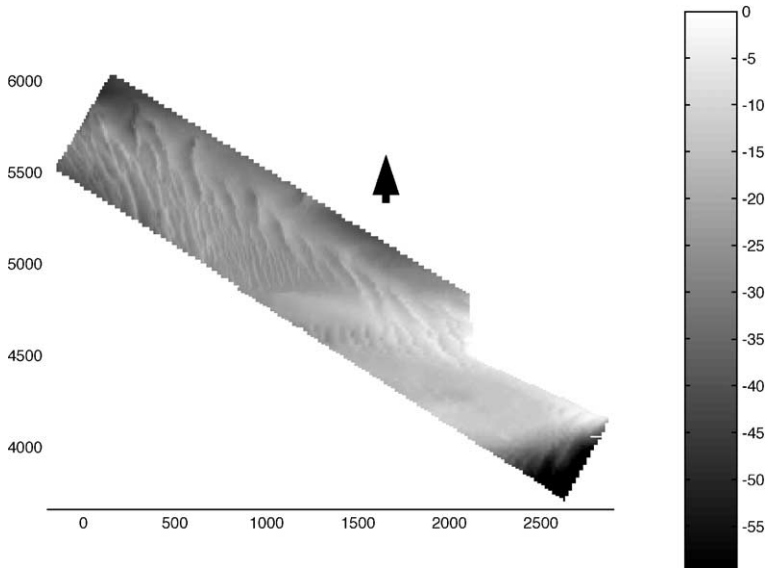

Fig. 3. The bathymetry measured in 1997. The bar gives the depth in metres. The arrow points north.

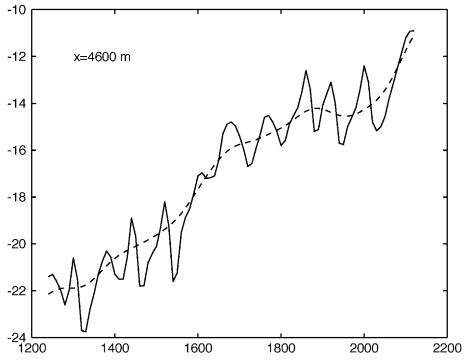

Fig. 5. The depth profile in the connection channel.

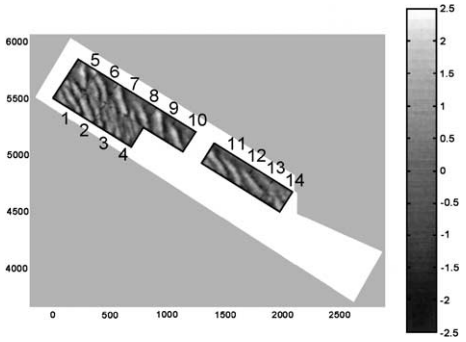

Fig. 7. The selected areas.

(Fig. 2), the bathymetry is dominated by the Inosakinotsugai shoal.

In several places in the Bisanseto Sea, sand waves are present (see Fig. 3). In general, these sand waves do not hinder navigation. On the Inosakinotsugai shoal and the immediate surroundings, however, the sand waves reduce the navigation depth. In the northern channel (see Fig. 4) near the shoal, over 3-m high sand waves reduce the navigation depth from 22 m to less than the required 19 m. In the connection channel over the shoal (see Fig. 5), the sand waves reduce the depth from about 15 m to less then the required navigation depth of 13 m.

Between 1981 and 1998, the upper parts of the sand waves were dredged in order to have a navigation depth of 22 and 15 m in the northern and connection channel, respectively. The regeneration process of the sand waves was followed during the next 10 years (see Katoh et al., 1998). Once a year, the depth was measured using echo sounding in an area of 500×2000 m. The data was stored with a resolution of 5×5 m. Fig. 3 shows the measured bathymetry of 1997. One can clearly see the shoal, just below the

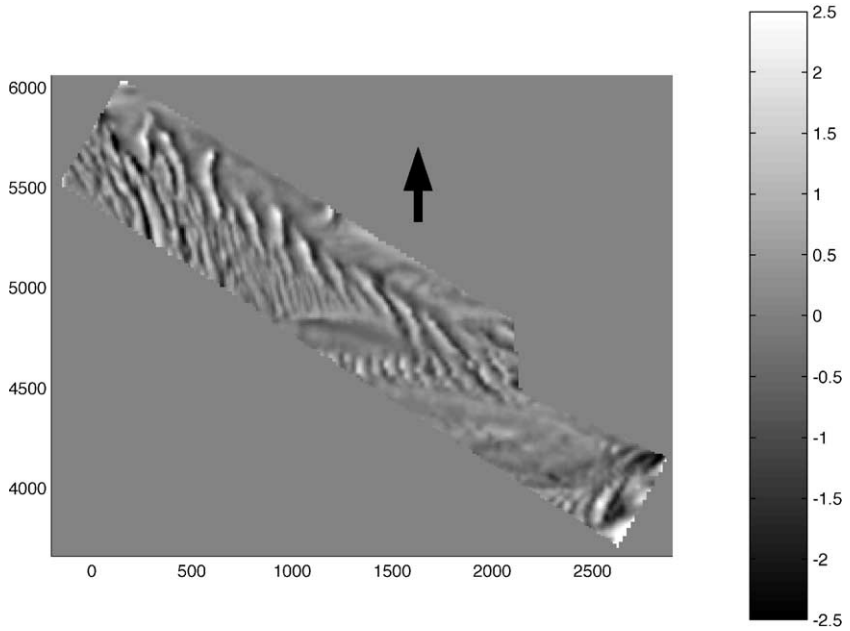

Fig. 6. The sand waves observed in 1997. The bars give the deviation from the mean depth in metres. The arrow points north.

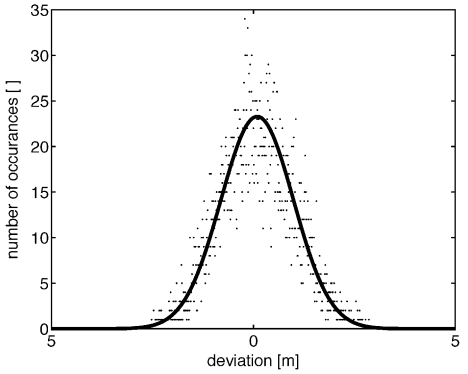

Fig. 8. The histogram of measured deviations from the mean bed level (dots) resembles a Gaussian distribution (line).

centre, and the sand waves in the northern channel in the upper part of Fig. 3.

To find the characteristics of the sand waves, the mean bathymetry was removed. A low-pass filter, with a large window (39 size Hamming window, which covers 200 m), removes all small-scale patterns to give the mean profile. Subtraction of this mean bathymetry from the original data gives the sand waves. Fig. 6 shows the resulting sand wave field of 1997.

From all 10 available data sets between 1985 and 1996, the sand wave fields are isolated in this way. To evaluate the growth of the waves, 14 areas (200×200 m) are selected (see Fig. 7). In these areas, the mean sand wave amplitude is estimated using the statistics of the measurements. The bathymetry is stored on a regular grid, and since the mean profile is removed, the average value of the filtered data is zero. Therefore, assuming sinusoidal sand waves, the mean amplitude A is equal to:

$$A = \sigma\sqrt{2} \tag{3}$$

in which σ is the standard deviation (in m) of the filtered data in a box. For the Bisanseto data, the assumption of sinusoidal waves is confirmed by the distribution, which is almost Gaussian (Fig. 8). The profiles given by Katoh et al. (1998) are a second confirmation. In the worst case, for asymmetric sawtooth waves, Eq. (3) would result in amplitude estimates that are 20% too small.

Fig. 9 shows the resulting amplitudes, nondimensionalized with the mean depth H, plotted against time.

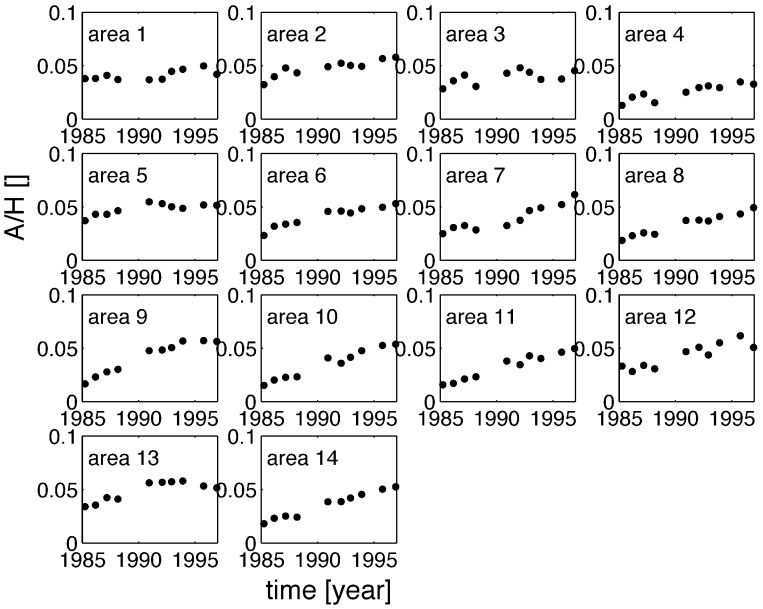

Fig. 9. The dimensionless amplitudes plotted against time.

3. Amplitude evolution model

Straightforward numerical simulation based on small-scale process descriptions is laborious and error-prone. Therefore, state-of-the-art research on this type of rhythmic morphological patterns is focused on linear and nonlinear stability analysis of idealized models (Vittori and Blondeaux, 1990; Schielen et al., 1993; Hulscher, 1996; Komarova and Hulscher, 2000; Komarova and Newell, 2000). Based on the findings in earlier work, Hulscher (1996) and Komarova and Hulscher (2000) assume that sand waves are perpendicular to the flow and that they are not influenced by geostrophic effects.

Therefore, modelling of sand waves is restricted to one horizontal and one vertical dimension. In this two-dimensional space, the turbulent flow is given by the Reynolds equations:

$$\frac{\partial \vec{u}}{\partial t}(\vec{u}\vec{\nabla})\vec{u} = -\frac{\vec{\nabla}p}{\rho} - \frac{\vec{\nabla}\vec{\tau}}{\rho} \tag{4}$$

$$\vec{\nabla}\vec{u} - 0 \tag{5}$$

where $\vec{\tau}$ is the Reynolds stress tensor, $\vec{u} = (u, w)$ is the turbulence-averaged velocity vector, as defined in Fig. 10. Furthermore, p is the total pressure $p=p' - \rho g(z-\zeta)$ and ρ denotes the mass density of the seawater. Following the ideas of Bagnold (1956), the bedload sediment transport q is given by a generic formula (Komarova and Hulscher, 2000; Komarova and Newell, 2000):

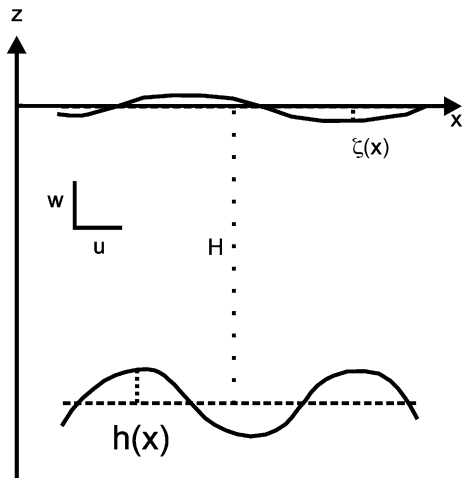

Fig. 10. Sketch explaining the definitions in the model of Komarova and Hulscher (2000), with mean water depth H, sand wave height $h(x, t)$, water surface deviations $\zeta(x, t)$ and flow vector $[u(x, z, t), w(x, z, t)]$.

$$q = \alpha|\tau_b|^b(\tau_b - \lambda\nabla h) \tag{6}$$

in which $\vec{\tau}_b$ denotes the bottom shear stress, λ is the downhill coefficient, b the nonlinearity parameter and α the proportionality parameter. Eq. (6) is a generic expression that reflects the influence of the two most important forces that act on the sediment grains. The first term represents the drag effect, the second the gravity component. Finally, continuity of sediment mass results in the bed evolution equation:

$$\frac{\partial z_b}{\partial t} = -\frac{\partial q}{\partial x} \tag{7}$$

in which z_b is the bed level relative to the mean depth. The model is closed by boundary conditions at the bottom and at the free surface and using a turbulence closure model.

An obvious solution to this model is a flat bed with a horizontally uniform tidal motion on top of it. This solution is here selected as the basic state. The equations allow for the development of a wide range of travelling periodic wave trains, for example, the ones comparable to migrating sand waves. Therefore, in the next step of the stability analysis, this basic state is perturbed by an infinite number of infinitesimally small sine waves:

$$\phi = \phi_o + \int_o^\infty \epsilon\phi_1(k)e^{ikx+\omega t}dk + \text{c.c.} \tag{8}$$

in which $\phi=(u, w, \zeta, z_b)$ and ϕ_o denotes its basic state. The small parameter ε guarantees that the imposed perturbations are small. Furthermore, k denotes the wave number of the sine waves and ω is the complex morphological wave frequency. According to Komarova and Hulscher (2000), ω depends on two physical parameters, the resistance parameter and the turbulent viscosity. If the growth rate (given by the real part of ω) is negative, the basic state is stable: the perturbations decrease in amplitude and disappear. If the growth rate is positive, the basic state is unstable: the perturbations start to grow, thus forming a rhythmic pattern.

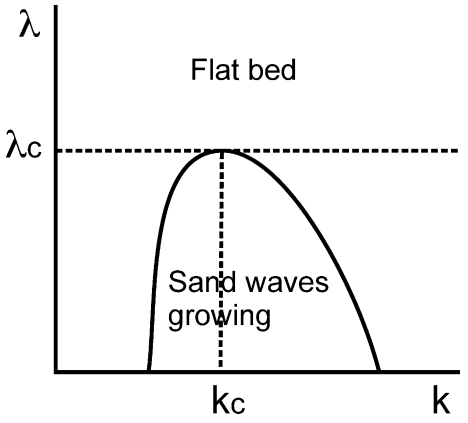

Fig. 11. Sketch of a typical neutral curve, separating the region with a stable basic state from the region with growing disturbances. λ is the control parameter; k gives the wave number of the perturbations.

Komarova and Hulscher (2000) substituted the perturbed basic state (Eq. (8)) into the scaled equivalent of Eqs. (4)–(6), linearized for small perturbations. Thus, they found a relationship between the complex wave frequency and the wave number. Using this relationship, one can determine whether the basic state is stable or unstable. As can be seen in Fig. 11, there is a range of waves with a positive growth rate, if $\lambda<\lambda_c$.

A nonlinear analysis results in a complex equation describing the behaviour of the sand waves. Komarova and Newell (2000) performed the nonlinear stability analysis for a 2DV tidal model. As a result, they found two coupled evolution equations of the Ginzburg–Landau type, which predicts sand waves superimposed on sand banks. If the large spatial modulations are neglected, this model reduces to the Landau equation.

Based on these findings, we assume that the growth of sand waves is described by the real Landau equation:

$$\frac{\partial A}{\partial \tau} = \alpha_0 A - \alpha_1 |A|^2 A \tag{9}$$

$$\tau = \frac{t}{T} \tag{10}$$

in which t is the real time and τ is the morphological time, defined by a long timescale T. The real variable A is the amplitude of the bed form:

$$h(x,t) = A(\tau)\cos kx + \text{h.o.t.} \tag{11}$$

where k is the wave number of the perturbation h (h.o.t. denote the higher order terms representing asymmetry). Finally, α_0, $\alpha_1>0$ are dimensionless parameters. Note that the migration of the sand waves is not taken into account. The simplification, to treat amplification apart from migration, is justified by the measured data from the Bisanseto Sea. Eq. (9) can easily be transformed to:

$$\frac{\partial A}{\partial \hat{\tau}} = A - \hat{\alpha}\,|A|^2 A$$

$$\hat{\tau} = \frac{t}{\alpha_0 T}$$

$$\hat{\alpha} = \frac{\alpha_1}{\alpha_0} \tag{12}$$

A genetic algorithm optimization routine estimates the model parameters $\hat{\tau}$ and $\hat{\alpha}$ from the measured data. These are the only parameters of interest, since we are interested in the changes in time of A. Note that parameter $\hat{\alpha}$ defines the maximum amplitude:

$$A(t=\infty) = \sqrt{\frac{1}{\hat{\alpha}}} = \sqrt{\frac{\alpha_0}{\alpha_1}} \tag{13}$$

4. Genetic algorithm

An optimization algorithm, Fletcher (1987) can find the best values of both the parameters and the initial state of the model relative to the measured data. Because of the nonlinearity of the model, gradient search algorithms are not very effective (Floudas and Pardalos, 1996). Therefore, we use a global optimization routine. A genetic algorithm, a stochastic search, is such a global optimization routine.

The algorithm is analogous to the evolution theory: 'In general, the fittest individuals of any population tend to reproduce and survive to the next generation, thus improving successive generations. However, inferior individuals can, by chance, survive and reproduce. Genetic algorithms have shown to solve linear and nonlinear problems by exploring all regions of state space and exponentially exploiting promising areas through mutation, crossover and selection operations applied to individuals in the population' (Michalewicz, 1994).

The genetic algorithm starts from a population of a randomly chosen initial guesses. Every member of the population is a combination of possible parameter values. Furthermore, every member receives a fitness coefficient. This coefficient depends on the difference between the measured bathymetry and the bathymetry estimated using the parameters of this member. From this initial guess, an iterative search is started (see Fig. 12).

In every iteration step, the members of the population are combined to create more members. This combining follows the rules of biological reproduction:

- two members combine parameters (genes) to give birth to one or more new members (crossover, comparable to sexual reproduction)
- one parameter of one of the members is changed to give one new member (mutation, comparable to asexual reproduction).

At the end of each step, only part of the population survives. The fittest members (parameter combinations that give the smallest difference between measured and modelled bathymetry) have a bigger chance to survive than members that result in less accurate bathymetry estimates do. This way the algorithm evolves to the best fit between model and data.

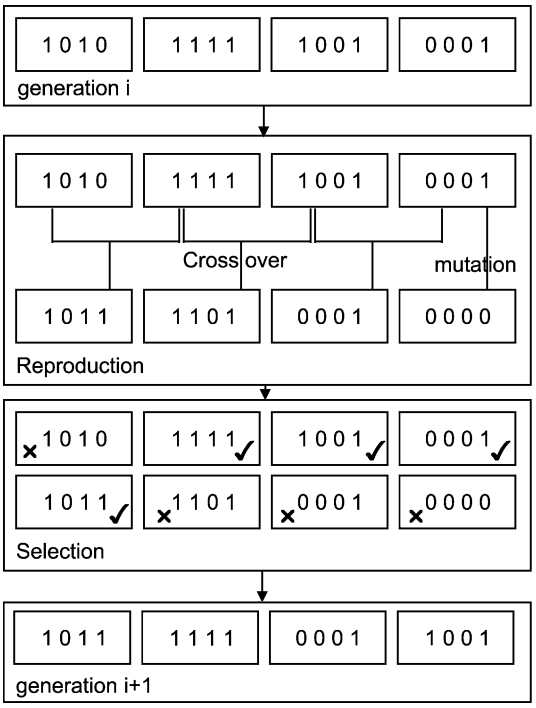

Fig. 12. Flow chart of the genetic algorithm. In the selection step, the ✓ denotes the surviving members, × denotes the extinct ones.

Although this optimization routine is very robust (it always finds a solution that is close to the optimal solution), the procedure can be repeated with new initial populations to exclude any remaining dependencies on the initial guess. In practice, this leads to marginal improvements.

More details can be found in Davis (1991), who gives an extensive discussion of genetic algorithms.

5. Hindcast of sand wave growth in the Bisanseto Sea

In the Bisanseto Sea, measurements have only been taken after one dredging operation. Consequently, it is difficult to design a distinctive test on the predictive capacity of the model. Yet, this data set is very useful to compare the model behaviour with the dynamics of real sand waves. The genetic algorithm is used to find those parameters that give the best agreement between the modelled wave heights and the measured wave heights at all points in time. The results in Fig. 13 show that the difference between the model and the data is considerably smaller than the noise in the signal (S.D. of the noise varies between 3% and 30% of the signal).

Fig. 14 shows the optimal parameter values of the model for all 14 parts. The timescale $\alpha_0 T$ is between 3.6 and 8.3 years (mean value 5.9 years, S.D. 1.73 year) This is remarkably constant given the complex flow over the shoal and the large variations in the sediment characteristics (Ozasa, 1974). These optimal values are of the same order as the theoretical values found by Hulscher (1996) and Gerkema (2000). However, in both theoretical derivations, numerical problems prevented the calculation of the parameter values in case of small sand waves, like in this area. Our approach does give an estimate of the timescale for such small sand waves.

The parameter $\hat{\alpha}$ appears to be related with the position on the shoal. On the south side (Areas 1–4), the magnitude of $\hat{\alpha}$ appears to be inversely proportional to the depth. This could be related to a decrease

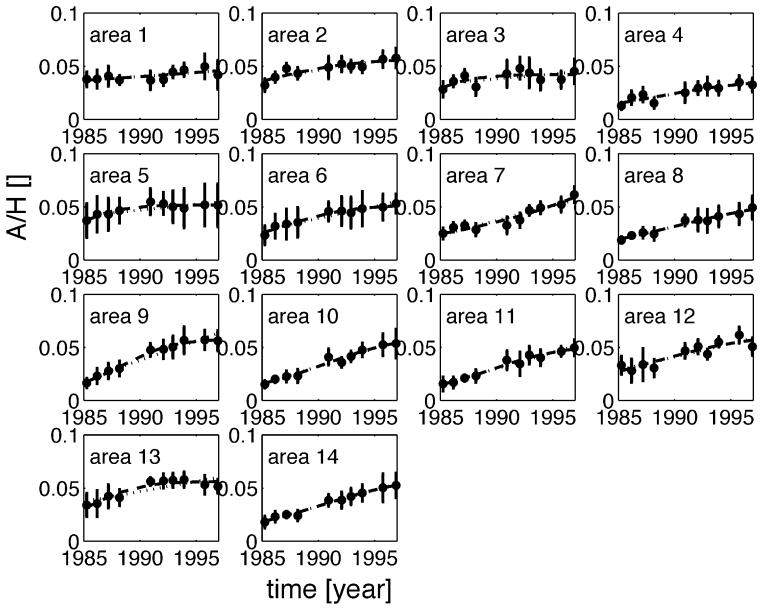

Fig. 13. Comparison between the amplitude measured in the Bisanseto Sea (dots), the growth according to the model (dashed lines) and a linear trend analysis (dotted lines). The vertical bars give the standard deviation of the measurements.

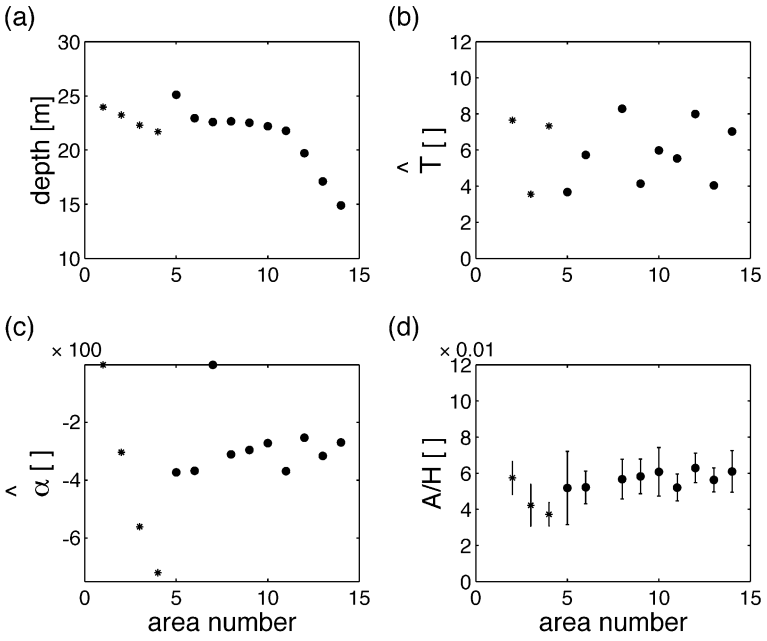

Fig. 14. Important parameters of the mode: (a) the mean depth H, (b) tuning parameter $\hat{T}$, (c) tuning parameter $\hat{\alpha}$ and (d) the resulting dimensionless sand wave amplitude for the 14 parts.

Table 1
Correlation between data and model compared to the correlation between the data and a linear trend model

Area	1	2	3	4	5	6	7	8	9	10	11	12	13	14
Model	0.67	0.91	0.68	0.91	0.93	0.98	0.96	0.98	0.99	0.98	0.98	0.91	0.95	0.99
Trend	0.67	0.90	0.57	0.90	0.79	0.96	0.94	0.98	0.97	0.98	0.98	0.90	0.82	0.99

of the flow velocities going east, a decrease of the water depth and an increase in the grain size of the sediment, which have been observed by Ozasa (1974). However, the absence of detailed information makes it impossible to draw any conclusions.

On the north side (Areas 5–14), its value is almost constant (mean −314, S.D. 46, which is equivalent to a undisturbed sand wave height of 11±1% of the water depth). On this side, there is no evidence that there is a significant relation with the water depth. This implies that the model assumptions in the theoretical derivations (Hulscher, 1996; Komarova and Hulscher, 2000; Komarova and Newell, 2000) hold for this area, even if the water depth is about 15 m.

The variation in $\hat{\alpha}$ is not undermining the model. In practice, the amplitude before dredging will be known. This amplitude determines the value of $\hat{\alpha}$ according to Eq. (13).

The optimization in Areas 1 and 7 result in values of $\hat{\alpha}$ equal to −1. This value implies that the final wave height would equal the water depth. This is unrealistic, which makes the results suspect. Therefore, the results have to be rejected. Note that this provides an internal security check on the prediction.

The correlation between the measured wave height and the model estimates is high (Table 1). As a test, the results are compared with a linear trend analysis (see Fig. 13). The model is an improvement with respect to this trend analysis for two reasons. Most importantly, it gives a finite amplitude, whereas the linear trend results in infinitely large sand waves when time increases. Moreover, even if the sand waves appear to be far from their maximum amplitude (Areas 7, 8, 10, 11, 14), the correlation with the measurements is higher for the model than for the linear trend.

6. Prediction of sand wave growth

As mentioned in Section 5, testing the predictive capacity is formally impossible due to the lack of predredging data. However, a first test of this capacity is possible. In some areas, the sand waves seemingly have reached their final amplitude. Here, we assume that this amplitude approximately equals the amplitude before dredging.

Using this assumption, a test case can be assembled. The hypothetical predredging sand wave height and three measurements after dredging are used to tune the model. After that, the model results are compared to the measured amplitudes.

Fig. 15 shows the results of Area 9. In this area, the sand waves appear to have reached the maximum height and they have been dredged far enough to make the test distinctive. In most other areas, except Area 12, the results are similar. However, the evolution of the sand waves is less strong, which makes the comparison less distinctive.

The agreement between the predicted and measured values is good (Fig. 15), the correlation of the prediction (0.99) is only marginally smaller than the hindcast value, given in Table 1. In this test, the advantage on the linear trend is quite visible. Whereas the model finds an finite amplitude, the trend finds ever growing sand waves.

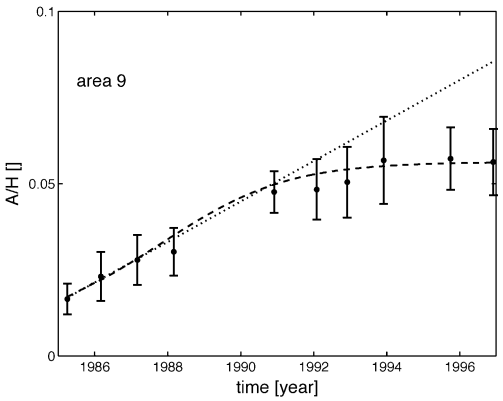

Fig. 15. Prediction of the sand wave growth in area 9 using the model (dashed line) and a linear trend analysis (dotted line), both based on a tuning on the first three measurements.

7. Model application

The results in this paper show that the proposed model, in combination with a genetic algorithm, gives a good representation of the process of sand wave growth in time. This makes it a useful tool for coastal management. Often, when a navigation channel crosses a sand wave field, the sand waves have to be dredged. After dredging, the sand waves regenerate. This process implies two problems. First, the bathymetry has to be monitored to check if the agreed navigation depth is secured. Second, one has to decide how deep the sand waves should be dredged.

For both problems, our model provides a decision support tool. Once the model has been tuned, it can estimate the growth process of the sand waves. From these estimates, one can estimate when the amplitude is likely to become critical to the navigation depth. Until that time, no expensive monitoring is necessary.

The model can also be used to optimize the dredging strategy. For different dredging depths, one can estimate the time it takes for the sand waves to return to the critical amplitude (see Fig. 16 for an example). Thus, it is possible to estimate the dredging frequency and the costs involved.

Another possible application is the recovery of sand waves in areas where sand is mined, like some parts of the North Sea. The mining can take place either by an overall lowering of the seabed, or by crest removal. Practical problems arising with offshore sand mining are the safety of buried infrastructure, such as pipelines and cables and the risk of exposure of polluted material or buried objects (mines or disposed material). The model can be used to support a decision on how to mine the sand, concentrated in deep pits or superficially over large areas.

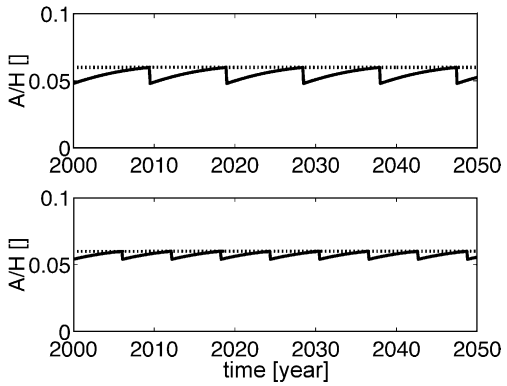

Fig. 16. The variation in time of the mean dimensionless amplitude A/h for two dredging strategies. Reduce the amplitude of the sand waves with 20% (top) and with 10% (bottom). It is assumed that the average depth remains unaltered, which is the case when dredged material is dumped in the troughs.

The approach would be even more useful, if the required number of surveys after dredging, now three surveys covering 2 years, could be reduced. For this purpose, the model parameters should be related to process related parameters, comparable to the work of Knaapen et al. (2001). The model properties are perfect for this purpose. However, such an improved procedure still requires further research.

8. Conclusions and discussion

The bed of Bisanseto channel is characterized by a shoal covered with sand waves. These sand waves reduce the navigation depth considerably. To increase the navigation depth, the sand waves have been dredged. After the dredging, sand waves reach their equilibrium height in approximately 10 years.

Based on existing literature, it may be assumed that the growth of sand waves can be modelled using a simple amplitude-evolution model based on the Landau equation. This assumption is confirmed by observations in this paper.

The combination of an amplitude-evolution model with measured data is a potentially useful tool for the maintenance of navigation channels through a sand wave field. If the model is tuned by a genetic algorithm, the growth process of the dredged sand waves can be reproduced well. The correlation between the model and the measurements is high. Furthermore, a first test shows that this model has predictive capacity.

The optimal model parameters are of the same order as could be expected from theory. This paper proposes an objective method to derive the timescale of sand waves. The timescale for sand wave growth equals the scale that is found in literature (± 10 years) (Hulscher, 1996; Dodd et al., in press).

In general, the optimal parameter values are almost uniform. This implies that the sand wave height is depth determined. However, on the south side of the

shoal, there is a trend in the values that could be related to variations in the water depth, grain size and flow velocities. The new approach described in this paper has three advantages over a linear trend analysis. First of all, the new approach fits better with the data. Second, it predicts a growth towards a finite amplitude. Third, the characteristics of the model are in agreement with the theoretical derivations (Hulscher, 1996; Komarova and Newell, 2000; Gerkema, 2000), which makes a combination of the theoretical work with our data driven model possible.

In the entrance channel to Rotterdam Harbour, individual sand waves are topped off when they become to large. No significant regeneration has been observed because so far only individual, extremely large sand waves have been topped off. In case the navigation depth would be increased, however, a larger part of the sand waves will be dredged. It is very likely that the sand waves in this area will then regenerate as well.

Acknowledgements

The authors like to thank Dr. Katoh of the Port and Harbour Research Institute of the Japanese Ministry of Transport for making the measured data available. Furthermore, we thank Mr. O. Scholl for his MSc project, which was related to this paper. The research described in this paper is partly funded by the Dutch Organization for Scientific Research (NWO) under project no. 620-61-349, and Technology Foundation STW, Applied Science Division of NWO and the Technology Programme of the Ministry of Economic Affairs (TCT-4466). This work is carried out in the framework of the EU project HUMOR (EVK3-CT-2000-00037) and the Delft Cluster project Eco-morphodynamics of the seafloor.

References

Aliotta, S., Perillo, G.M.E., 1987. A sand wave field in the entrance to Bahia Blanca estuary. Marine Geology 76, 1–14.

Amos, C.L., King, E.L., 1984. Bedforms of the Canadian Eastern seaboard: a comparison with global occurrences. Marine Geology 57, 167–208.

Bagnold, R.A., 1956. The flow of cohesionless grains in fluids. Proceedings of the Royal Society of London 249 (A 946), 235–296.

Bénard, H., 1900. Les tourbillons cellulaire dans une nappe liquide. Revue Génerale Pures et Appliques 11, 1261–1271.

Boggs, S., 1974. Sand wave fields in Taiwan Straight. Geology 2, 251–253.

Bokuniewicz, H.J., Gordon, R.B., Kastens, K.A., 1977. Form and migration of sand waves in a large estuary, long island sound. Marine Geology 24, 185–199.

Davis, L., 1991. The Handbook of Genetic Algorithms. Van Nostrand-Reinhold, New York.

DiPrima, R.C., Swinney, H.L., 1981. Instabilities and transition in flow between concentric cylinders. In: Swinney, H., Gollub, J.P. (Eds.), Hydrodynamic Instabilities and the Transition to Turbulence. Topics in Applied Physics, vol. 45. Springer-Verlag, New York, pp. 139–180.

Dodd, N., Blondeaux, P., Calvete, D., De Swart, H.E., Falques, A., Hulscher, S.J.M.H., Rozynski, G., Vittori, G., 2001. The use of stability methods for understanding the morphodynamical behaviour of coastal systems. Journal of Coastal Research, in press.

Field, M.E., Nelson, C.H., Caccione, D.A., Drake, D.E., 1981. Sand waves on an epicontinental shelf: Northern Bering Sea. Marine Geology 42, 233–258.

Fletcher, R., 1987. Practical Methods of Optimization. Wiley, Chichester.

Floudas, C.A., Pardalos, P.M. (Eds.), 1996. State of the Art in Global Optimization. Kluwer Academic Publishers, Dordrecht. 651 pp.

Fredsøe, J., Deigaard, R., 1992. Mechanics of coastal sediment transport. Technical report, Institute of Hydrodynamics and Hydraulic Engineering, Technical University of Denmark.

Gerkema, T., 2000. A linear stability analysis of tidally generated sand waves. Journal of Fluid Mechanics 417, 303–322.

Harris, P.T., 1988. Sediment, bedforms and bedload transport pathways on the continental shelf adjacent to Torrres Strait, Australia–Papua New Guinea. Continental Shelf Research 8 (8), 979–1003.

Hulscher, S.J.M.H., 1996. Tidal-induced large-scale regular bed form patterns in a three-dimensional shallow water model. Journal of Geophysical Research 101 (C9), 20727–20744.

Hulscher, S.J.M.H., Van Den Brink, G.M., 2001. Comparison between predicted and observed sand waves and sand banks in the north sea. Journal of Geophysical Research 106 (C5), 9327–9328.

Huntley, D.A., Huthnance, J.M., Collins, M.B., Liu, C.-L., Nicholls, R.J., Hewitson, C., 1982. Hydrodynamics and sediment dynamics of North Sea sand waves and sand banks. Philosophical Transactions of the Royal Society of London 4, 79–99.

Ikehara, K., Kinoshita, Y., 1994. Distribution of subaqueous dunes on the shelf of Japan. Marine Geology 120, 75–87.

Katoh, K., Kume, H., Kuroki, K., Hasegawa, J., 1998. The development of sand waves and the maintenance of navigation channels in the Bisanseto Sea. Coastal Engineering '98. ACSE, Reston, VA, pp. 3490–3502.

Knaapen, M.A.F., Hulscher, S.J.M.H., De Vriend, H.J., Van Harten, A., 2001. Height and wave length of alternate bars in rivers: modelling vs. laboratory experiments. Journal of Hydraulic Research 39 (2), 147–153.

Komarova, N.L., Hulscher, S.J.M.H., 2000. Linear instability mechanics for sand wave formation. Journal of Fluid Mechanics 413, 219–246.

Komarova, N.L., Newell, A.C., 2000. Nonlinear dynamics of sand banks and sand waves. Journal of Fluid Mechanics 415, 285–312.

Kuramoto, Y., 1984. Chemical Oscillations, Waves and Turbulence. Springer-Verlag, New York.

Lanckneus, J., De Moor, G., 1991. Present-day evolution of sand waves on a sandy shelf bank. Oceanologica Acta 11, 123–127.

Landau, L.D., Ginzburg, V.L., 1965. On the theory of superconductivity. Paper no. 73.

Langhorne, D.N., 1973. A sand wave field in the outer Thames estuary, Great Britain. Marine Geology 14 (2), 129–143.

Ludwick, J.C., 1972. Migration of tidal sand waves in Chesapeake Bay entrance. In: Swift, D., Duane, D., Pilkey, O. (Eds.), Shelf Sediment Transport: Process and Pattern. Dowden, Hutchinson and Ross, Stroudsburg, PA, pp. 377–410.

Michalewicz, Z., 1994. Genetic Algorithms+Data Structures= Evolution Programs. AI Series. Springer-Verlag, New York.

O'Conner, B.A., 1992. Prediction of seabed sand waves. In: Partidge, W. (Ed.), Computer Modelling of Seas and Coastal Regions. Computational Mechanics Publishers, Southampton, pp. 322–338.

Ozasa, H., 1974. Field investigation of large submarine sand waves. Coastal Engineering in Japan 17, 155–184.

Schielen, R.M.J., Doelman, A., De Swart, H.E., 1993. On the nonlinear dynamics of free bars in straight channels. Journal of Fluid Mechanics 252, 325–356.

Stewartson, K., Stuart, J.T., 1971. A non-linear instability theory for a wave system in plane Poiseuille flow. Journal of Fluid Mechanics, 48.

Stride, A.H. (Ed.), 1982. Offshore Tidal Sands: Processes and Deposits. Chapman & Hall, London, 222 pp.

Terwindt, J.H.J., 1971. Sand waves in the Southern Bight of the North Sea. Marine Geology 10, 51–67.

Van de Meene, J.W.H., Van Rijn, L.C., 2000. The shoreface-connected ridges along the central Dutch coast: Part 1. Field observations. Continental Shelf Research 20, 2295–2323.

Van Maren, D.S., 1998. Sandwaves, a state-of-the-art review and bibliography. Technical report, Ministry of Transport, Public Works and Water Management, North Sea Directorate, Rijswijk, The Netherlands.

Vittori, G., Blondeaux, P., 1990. Sand ripples under sea waves: Part 2. Finite-amplitude development. Journal of Fluid Mechanics 218, 19–39.